Desalination and Water Treatment
www.deswater.com

doi: 10.1080/19443994.2015.1096835

57 (2016) 18573–18587
August

Taylor & Francis
Taylor & Francis Group

Technical evaluation of simple condenser devices for a bubble column desalinator

Mario Schmack*, Goen Ho, Martin Anda

School of Engineering and Information Technology, Murdoch University, 90 South Street, Murdoch 6150, Western Australia, Tel. +61 8 9360 6399; email: M.Schmack@murdoch.edu.au (M. Schmack), Tel. +61 8 9360 2167; email: G.Ho@murdoch.edu.au (G. Ho), Tel. +61 8 9360 6123; email: M.Anda@murdoch.edu.au (M. Anda)

Received 28 May 2015; Accepted 13 September 2015

ABSTRACT

Several simple vapour cooling and pre-condensing concepts were assessed for the purpose of mitigating bubble column vapour temperatures, a critical aspect for the development of a bubble column driven greenhouse desalination system. Particular emphasis was on low-energy demand of the devices, ease of manufacture, low investment cost and technical and operational appropriateness for local people in remote places. Under laboratory conditions, the copper tube type I and II concepts achieved water recovery rates of between 65 and 75%. The water-tank cooled tube achieved 83% condensate recovery, albeit at the cost of large cooling water requirements, whereas the air cooled and *passive sleeve*-cooled bubble condenser columns achieved condensate recovery rates of at least 50% under favourable ambient conditions. A "self-cooling" effect was observed for the *passive sleeve* columns that could perhaps be tailored to produce small quantities of potable water in hot and arid regions. The *effectiveness*–NTU method was used to allow for a meaningful comparison between the devices. While the majority of the tested concepts represented a "single-stage" approach to the humidification–dehumidification cycle, it is stressed that a well-designed latent heat recovery system would be crucial for the economic viability of a bubble greenhouse.

Keywords: Bubble column evaporation; Bubble-greenhouse; Passive condenser; Seawater desalination; Brackish water desalination

1. Introduction

This work was motivated by the need to mitigate the vapour temperature from a bubble column evaporator, as a means of humidifying a conceptual bubble greenhouse. The novel greenhouse-based desalination system aims at utilising low-key devices with minimal technical complexity and energy demand. Bubble column technology has recently gathered attention as a prospective method for water desalination, both for humidifying [1] and dehumidifying [2] purposes. While technically advanced multi-stage bubble column condensers have reached a level of maturity that suggests commercialisation in the near future [3–5], the humidification–dehumidification (HD) concepts investigated here employ a single-stage bubble column evaporator in combination with several easy-to-make condensation devices, under the important proviso of being a low-tech method that is operational by local

*Corresponding author.

people in remote regions [6]. As such, this paper provides important insights into steam cooling dynamics for the conceptual bubble-greenhouse desalination system and identifies future research areas.

Solar stills are the most basic exponents of small-scale desalination systems, utilising the quintessential principles of solar thermal desalination. Some of their key advantages are that they are very simple, hardy and easy to maintain and repair by local people with limited technical means [7]. The idea to upscale the solar still concept by integrating large evaporation basins into a crop producing greenhouse has been around for some time [8]. A considerable number of studies on different still-greenhouse designs are available in the literature [9–12]. In general terms, the aim is to tailor and optimise the HD process inside a greenhouse, while making use of the structural components of the greenhouse itself, primarily as a condensing surface. However, based on the necessity to capture large amounts of heat from solar radiation as the driver for basin water evaporation, a crucial aspect in this concept is the risk of overheating the greenhouse and the resulting risk to plant survival.

An alternative method of humidification is realised in the Seawater Greenhouse. Here, surface seawater is trickled down porous evaporators that are made from a cardboard honeycomb lattice, for the dual purposes of feed water vaporisation and greenhouse temperature control [13]. While the greatest overall effect on condensate productivity and energy efficiency is determined by the dimensions of the greenhouse [14], the condenser design in seawater greenhouses is recognised as one of the main bottlenecks in the commercialisation of the technology [15]. Importantly, the evaporation rate of the cardboard honeycomb evaporator is linked to and thus, limited by ambient temperature conditions.

Owing to the relationship between saturated water vapour density and air temperatures [16], the higher process temperatures achievable with a bubble column evaporator can accomplish significantly larger evaporation rates. The process works by pumping a continuous stream of air from below through a column containing salty water. The unusual property of salt water to inhibit air bubble coalescence facilitates the performance of the bubble column with a high volume fraction of small air bubbles, continuously colliding but not coalescing [17]. In contrast to solar basin stills or flash distillation, where essentially only the surface of the liquid comes in contact with the air above, the bubble column produces a manifold liquid/air interface and as a result, a high exchange rate of water molecules from liquid to gas phase can be achieved.

While the higher evaporation rates of a bubble column over a conventional Seawater Greenhouse evaporator promote it as an alternative source for greenhouse desalination, the high vapour temperature —if left unmitigated—is problematic for plant survival. Crucially therefore, previous to greenhouse humidification it is essential to cool the vapour temperature to an acceptable level. This can be achieved by linking bubble column and greenhouse with a pre-cooling device, which has the added benefit of recovering a significant amount of condensate prior to greenhouse humidification. As the vapour stream is cooled down, the saturated vapour pressure remains at a maximum (i.e. 100% humidity), providing the greenhouse with a humidified environment that is conducive to crop production under a strongly reduced plant water demand [18].

For a conventional water condenser, the rate of condensation and thus, the net gain of desalinated water, are principally governed by the temperature difference between the warm vapour-saturated carrier medium (e.g. air) and the cooler condensing surface. The condensing surface in turn is kept cooler by the medium opposite (e.g. ambient air or cooling water). In this way, the condensing surface essentially acts as a physical barrier for matter, however, it allows for thermal energy (heat) contained in that matter to pass through. Condenser materials with a high thermal conductivity such as copper sheet excel at releasing heat through a process known as conduction [19]. The larger the temperature difference between inside and outside, the more and quicker heat is removed at the condenser surface. As a consequence, nearby water molecules are forced into a reduced energy state, expressed as a change from vapour to liquid water. As more and more water molecules condense, droplets and ultimately large drops of desalinated water form and can be collected [20].

The work presented here investigates several "simple-to-make" vapour cooling devices. The principal research question is how to achieve sufficient vapour cooling under a number of important provisos such as low-energy demand, low environmental impact, cost efficiency, durability and ease of maintenance. Besides their vapour cooling potential, the devices function as pre-condensing elements and their condensation production rates form an important part of the assessment. In its most basic expression, the vapour cooling concept explores several surface-type condensation devices in the form of copper tubes that operate under ambient air-cooled conditions or are installed inside a water-filled passive cooling tank. The pairing of two separate bubble columns into an evaporation–condensation module represents a unique and novel

approach to the HD challenge. A quantitative assessment of the water production capability is presented to demonstrate the potential of this concept.

2. Materials and methods

2.1. Evaporator design

The bubble column evaporator was manufactured from a clear Perspex cylinder of 500 mm height and 120 mm internal diameter. A 40–100 μm pore size glass sinter was sealed into the column with commercially available two-component glue. Top and bottom covers were attached and sealed with commercial Roof & Gutter Silicone. During operation, the lower part of the column was heated by an internal plastic tube heating spiral, fed from a water bath with a feed temperature of 70˚C. This resulted in a steam outlet temperature of around 55˚C, the maximum temperature practically achievable with this particular experimental set-up. Based on the exponential rise of water vapour density with temperature [16], the evaporation rate in a bubble column increases significantly with rising process temperatures, thus achieving higher output rates with smaller vessels. While the higher steam temperatures require mitigation previous to greenhouse humidification, a strongly improved "water production rate per infrastructure cost ratio" justifies the steam cooling expenditure, provided the cooling method is simple, effective and of low cost in terms of energy use and infrastructure.

The bubble column was filled with 2 L of sodium chloride (NaCl) salt solution with a concentration similar to seawater (35,000 ppm). During individual experiments, the evaporation chambers were not replenished, leading to a gradual salinity increase of about 15% above starting levels (40,500 ppm). Compressed air was continuously pumped through an inlet hose and through the glass sinter from below at a rate of 13.5 L min^{-1}, creating a high density of fine air bubbles. Due to a property of seawater, bubble coalescence was inhibited and the oscillating rise of bubbles resulted in a large and constantly renewed gas/water interface and thus, a uniform and efficient exchange of water vapour into the bubbles [17]. From an outlet hose on the column top, the heated vapour stream was channelled into the respective cooling devices. During the experiments, sheets of flexible foam were used to insulate the bubble column evaporator and the heating pipes, in order to prevent heat loss to the ambient air.

2.2. Vapour cooling concepts

Four types of cooling concepts were studied. These were air-cooled copper tubes (A), tank water-cooled copper tube (B), water-cooled glass column bubble condensers (C) and air-cooled and water-cooled copper column bubble condenser (D).

2.2.1. Copper cooling tube type I and II

The cooling tubes type I and II consisted of a section of commercially available annealed copper tube. Tube dimensions, experimental airflow rate and the resulting vapour residence times are given in Table 1. Thermocouples (PTFE type K/T.M. Electronics) were placed in pairs at defined locations (Table 1) to measure the rate of heat exchange through the copper wall as well as the lengthways temperature drop. Additional thermocouples were used to measure evaporator column temperature and heating coil inlet and outlet temperatures. Data loggers (HOBO-ware/Onset Computer Corporation) were used to measure temperature and humidity at the cooling tube exhaust, the compressed air inlet and of the ambient air. The tubes were directly attached to the bubble column vapour outlet and positioned with a gentle downwards slope (approximately 5%), to allow for condensation to flow out by gravity and to be collected and weighed for data collection. Passive tube cooling was induced by the temperature difference between the vapour stream and the ambient air.

2.2.2. Copper cooling tube type II in temperature gradient water tank

For this method, a plastic barrel filled with 160 L of water was used as a passive cooling device (Fig. 1). A section of annealed copper tube was coiled inside the cooling tank at a downward angle, to promote condensate outflow by gravitational force. Inside/outside pairs of thermocouples were placed near the copper tube inlet and outlet to determine the amount of heat released into the tank. Two additional thermocouples were placed inside the cooling tank, at 50 mm above tank bottom and 50 mm below the cooling water surface, to assess the developing tank temperature gradient and the thermal inertia relationship of the components.

2.2.3. Glass bubble column condenser

The bubble column condenser was manufactured from a sintered glass chromatography column with a

Table 1
Dimensions and experimental parameters of individual vapour cooling concepts

	Length (m)	Internal diameter (mm)	Volume (L)	Airflow rate (L min^{-1})	Residence time (s)	Thermocouple placement	Cooling method
Copper cooling tube type I	3	5	0.06	13.5	0.3	Inside/outside pairs near tube inlet and outlet	Ambient air
Copper cooling tube type II	3	10.9	0.28	13.5	1.2	Inside/outside pairs near tube inlet and outlet	Ambient air
Copper tube type II in water tank	3	10.9	0.28	13.5	1.2	Inside/outside pairs near tube inlet and outlet	Water tank
Glass bubble column condenser	0.4	42	0.55	13.5	2.5	Inside/outside pairs (bottom, mid and top)	Water sleeve
Copper bubble column condenser	0.4	40	0.48	13.5	2.1	Inside/outside pairs (bottom, mid and top)	Water sleeve

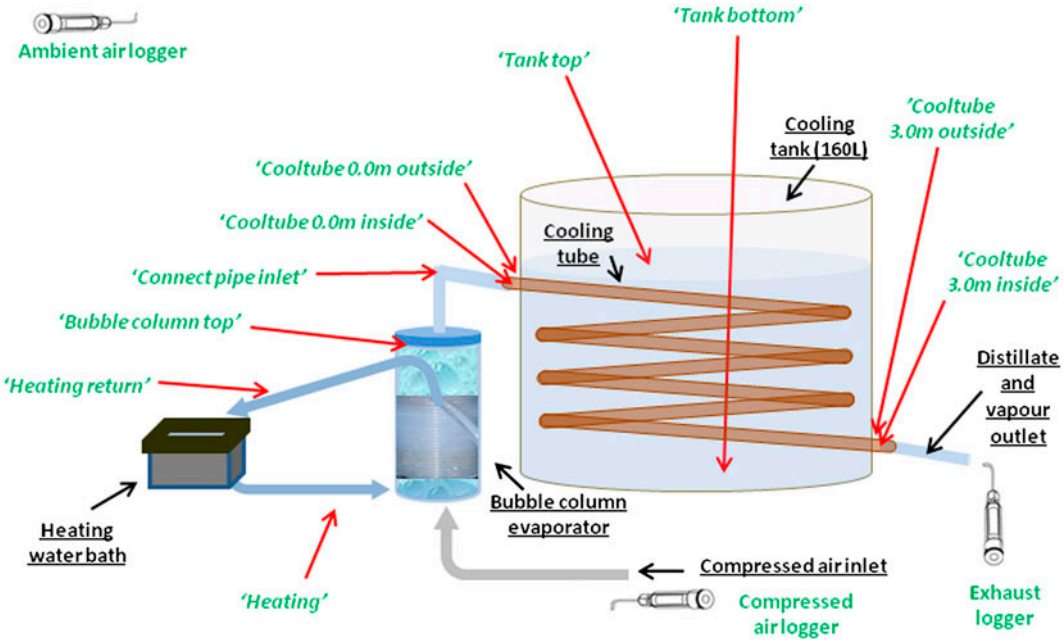

Fig. 1. Experimental design and sensor placement for the temperature gradient water tank experiments.

pore size of 40–100 μm (herewith termed *core*), sleeved by a section of commercially available 90 mm PVC stormwater pipe (*sleeve*), that allowed for cooling water to be contained (Fig. 2). The core column was filled to the top with desalinated water. Excess condensate that was constantly produced by the process was collected through an overflow outlet and determined by weight. The connection pipe between the evaporator column and the condenser column was shielded with insulation tubing in order to eliminate heat loss and unwanted condensation in this section as much as possible.

Pairs of thermocouples were placed at defined locations to measure the temperatures of core water and cooling water contained in the sleeve (Fig. 2). Overall, for assessment of the glass column condenser concept a series of experiments with varying cooling regimes were performed. *Active cooling* (or *active sleeve*) of the system was achieved by circulating cold water through a plastic tube coiled inside the sleeve. The

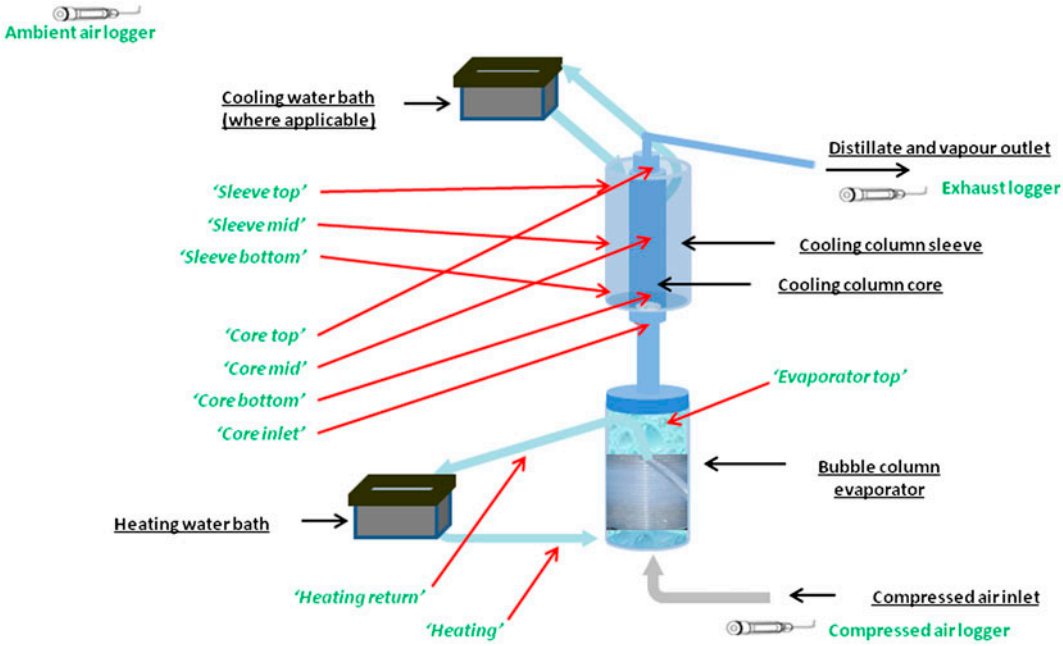

Fig. 2. Experimental design and thermocouple sensor placement (red arrows) for the glass cooling column experiments; sensors inside the core for monitoring vapour temperature changes; sensors inside the sleeve for monitoring cooling water temperature changes.

cooling level was controlled by the rate of cold water circulation. *Moderate cooling* was achieved by a slower circulation rate and with increased cold water circulation, *strong cooling* was realised. Additionally, several *passive sleeve* (*no cooling*) experiments were carried out, where the sleeve contained "cooling" water that was however not actively cooled by cold water circulation.

2.2.4. Copper bubble column condenser

This version of the stacked bubble cooling column consisted of the lower part of a sintered chromatography column with a section of copper tube attached. For this concept, several experiments were carried out with and without a sleeve. The un-sleeved cooling column was cooled by ambient air. For the sleeved version, a section of PVC pipe was fitted similar to the glass column described above (Fig. 2). The water contained in the *passive sleeve* was not cooled by cold water circulation. Thermocouple and humidity logger placement corresponded with the glass column experiments.

2.3. Experimental setup

Previous to all experiments the thermocouples were calibrated, using a precision alcohol thermometer (20–30 ± 0.02˚C). The humidity loggers were group tested in a steam chamber for their accuracy, particularly in the extreme upper region of maximum saturation. The rotameter used to measure airflow rate (Fisher Controls 25 ± 1 L) was calibrated through a volume displacement device. At the start of each experiment, two litres of NaCl salt solution were prepared and adjusted to a TDS concentration of 35,000 ppm with a conductivity meter (Hanna Instruments HI8733) and transferred into the bubble column evaporator.

Once the system had established steady state conditions as represented by thermocouple measurements, three one-hour measurement blocks for bubble column weight reduction (from saltwater evaporation) and condensate production were obtained using electronic scales (A&D Limited HW-15 K, 15,000 ± 1 g and A&D Limited GF 2000, 2,100 ± 0.1 g). Temperature and humidity readings from thermocouples and loggers were used to calculate the expected theoretical amount of evaporation and condensation per time unit, as governed by psychrometric law. Manual measurements of water bath temperature and cooling water temperature (where applicable) and heating flow rate and cooling flow rate (where applicable) were recorded. At the end of each experiment, water volume and conductivity of the column brine content and condensate conductivity were recorded.

2.4. Equations and parameters

Specific heat capacity:

$$Q = m \times C \times \Delta T \tag{1}$$

where Q is the rate of heat transfer (amount of heat energy gained or lost by substance) in kJ s^{-1}, m is the mass flow rate per time in kg s^{-1}, C is the specific enthalpy of condensation (heat capacity) in kJ kg^{-1} C^{-1} and ΔT is the temperature change in ℃.

Logarithmic mean temperature difference by LMTD method:

$$\Delta T_{\text{mean}} \equiv \text{LMTD} = (\Delta T_{\text{out}} - \Delta T_{\text{in}})/\ln(\Delta T_{\text{out}}/\Delta T_{\text{in}}) \tag{2}$$

where $\Delta T_{\text{in,parallel flow}} = t_{\text{h,in}} - t_{\text{c,in}}$ (inlet hot and inlet cold stream in ℃), $\Delta T_{\text{out,parallel flow}} = t_{\text{h,out}} - t_{\text{c,out}}$ (outlet hot and outlet cold stream in ℃), $\Delta T_{\text{in,counter flow}} = t_{\text{h,in}} - t_{\text{c,out}}$ (inlet hot and outlet cold stream in ℃) and $\Delta T_{\text{out,counter flow}} = t_{\text{h,out}} - t_{\text{c,in}}$ (outlet hot and inlet cold stream in ℃).

Overall heat transfer coefficient:

$$U = Q/A \times \Delta T_{\text{mean}} \tag{3}$$

where A is the surface area in m^2.

Energy balance in a single phase heat exchanger:

$$m_{\text{h}} \times C_{\text{h}} \times (T_{\text{h,in}} - T_{\text{h,out}}) = m_{\text{c}} \times C_{\text{c}} \times (T_{\text{c,out}} - T_{\text{c,in}}) \tag{4}$$

where m_{h} and m_{c} are the mass flow rates of the hot and cold fluid, respectively, in kg h^{-1}, C_{h} and C_{c} are the mass heat capacities of the hot and cold fluid, respectively, in kJ kg^{-1} C^{-1}, $T_{\text{h,in}}$ and $T_{\text{h,out}}$ are the inlet and outlet temperatures on exchanger hot side, respectively, in ℃ and $T_{\text{c,in}}$ and $T_{\text{c,out}}$ are the inlet and outlet temperatures on exchanger cold side, respectively, in ℃.

Enthalpy of moist air (sum of latent and sensible heat):

$$h = c_{\text{pa}} \times T + x_{\text{s}}[c_{\text{pw}} \times T + h_{\text{we}}] \tag{5}$$

where c_{pa} is the specific heat capacity of air (1.006 kJ kg^{-1} $℃^{-1}$), T is the air temperature (in ℃, relative to zero), x_{s} is the humidity ratio at saturation in kg of water per kg of air, c_{pw} is the specific heat of water vapour at constant pressure (1.875 kJ kg^{-1} $℃^{-1}$) and h_{we} is the evaporation heat of water at 0 ℃ (2,501 kJ kg^{-1}).

Effectiveness:

$$\varepsilon = C_{\text{h}} \times (T_{\text{h,in}} - T_{\text{h,out}})/C_{\min} \times (T_{\text{h,in}} - T_{\text{c,in}}) \tag{6}$$

where $C_{\min}$ is the smaller value of C_{h} (hot stream) and C_{c} (cold stream).
Number of transfer units (NTU):

$$\text{NTU}_{\text{counter-flow}} = [1/(C_{\text{ratio}} - 1)] \times \ln[(\varepsilon - 1)/(\varepsilon \times C_{\text{ratio}} - 1)] \tag{7}$$

$$\text{NTU}_{\text{parallel-flow}} = -\ln[1 - \varepsilon(1 + C_{\text{ratio}})]/(1 + C_{\text{ratio}}) \tag{8}$$

where

$$C_{\text{ratio}} = C_{\min}/C_{\max}$$

Overall heat transfer coefficient:

$$U = \text{NTU} \times C_{\min}/A \tag{9}$$

where A is the surface area in m^2.

3. Results and discussion

3.1. Bubble column evaporation

The fine sinter with a pore size of less than 100 μm produced a small bubble diameter (1–3 mm) and a large ratio of air bubbles to water volume, some of the key parameters that influence the diffusion of water into the air bubbles [21]. Consequently, the fine bubble size produced by the evaporator prototype directly translates into a shorter travel distance for equilibrium vapour pressure to occur. Throughout the experiments, height of the air bubble and water mixture was kept to 200 mm which was sufficient for achieving maximum saturation. In all experiments, the bubble column evaporator produced steady evaporation rates of 80–86 ml per hour, well correlated with expected theoretical values as determined by psychrometric chart.

While many factors such as water temperature, headwater difference and air velocity strongly influence humidification efficiency [22], the effect of rising salinity on the evaporation rate has, to our knowledge, not been previously assessed. For NaCl salt, bubble coalescence inhibition begins at a concentration above 4,600 ppm. Therefore, the bubble column evaporator can operate under brackish water salt composition scenarios of around 5,000 ppm upwards. At the upper

range, the evaporation figures remained constant within 80–86 ml per hour throughout the three-hour measurement blocks, despite the steady salinity increase that occurred due to the particularities of the experimental design. As the evaporation rate appeared unaffected by the increasing salt concentration, it was concluded that higher salinities, at least up to 40,500 ppm, would not reduce humidification efficiency.

3.2. Cooling concepts

3.2.1. Copper cooling tube type I and II

A simple approach to vapour temperature reduction was investigated by channelling the vapour stream directly through a length of copper tube that would be cooled passively by ambient air. Generally, the principal factors that influenced the cooling rate were (a) the temperature difference between bubble column vapour and the cooling medium ambient air and (b) the length of the cooling tube and the resulting vapour residence time. The main differences between type I and type II tubes were their wall thickness (0.55 mm vs. 0.9 mm) and their internal diameter (5 mm vs. 10.9 mm) which directly factored into vapour residence time (0.5 s vs. 2.2 s).

While the larger diameter of tube type II resulted in a four times longer residence time under the unchanged airflow regime, after correcting for ambient temperature, there was only a slightly stronger cooling effect of 0.7˚C compared to tube I. This translated into 56.5 ml of condensate production for type II vs. 53.8 ml for type I tube. A second factor influencing condensate productivity was the difference in total surface area of the tubes (0.12 m^2 for tube II vs. 0.06 m^2 for tube I). In order to allow for a meaningful comparison, the heat transfer rate (Q) for both tube types was calculated (Eq. (1)) as 0.0115 kJ s^{-1} (type I) and 0.0114 kJ s^{-1} (type II). The overall heat transfer coefficient (U) of compact single-phase heat exchangers (counter and parallel flow) is determined by a non-linear function, known as the logarithmic mean temperature difference, or LMTD method. Using Eq. (2), a LMTD of 12.0˚C for tube type I and 12.2˚C for tube type II was calculated. The overall heat transfer coefficient (Eq. (3)) for type I was then calculated as 16 W m^{-2} ˚C^{-1} and for type II as 7.8 W m^{-2} ˚C^{-1}, likely reflecting the different tube wall thicknesses of 0.55 mm for type II vs. 0.9 mm for type I tube.

These findings suggested the likely interplay of several factors being responsible for the relatively similar water production rate of the tubes. The twice as large heat transfer coefficient (type I) was counteracted by the four times larger residence time (type II), both being masked by the diffusion resistance effect that occurs in surface-type condensers [23]. It was therefore concluded that the thin-walled type I tube would be more effective as a passive vapour pre-cooling method under favourable ambient temperature conditions such as those experienced during the experiments. In regards to incorporating a tube-type cooling component into a conceptual bubble-greenhouse system, the use of type I tube would translate into considerable material savings.

3.2.2. Copper cooling tube type II in temperature gradient water tank

The latent heat of vaporisation per kilogram of pure water at 100˚C is around 2,258 kJ. While this figure slightly decreases with an increase in salinity (at 35,000 ppm it is about 2,180 kJ), thermal evaporation of saline water is very energy intensive. Unless a bubble column desalination system utilises a waste heat source from industrial processes [17], effective recovery of latent heat becomes a crucial aspect of its economic viability. By incorporating a large cooling water tank (160 L) as a heat collector, the tube cooling concept aimed to assess the potential for latent heat recovery in a technologically undemanding manner. Due to the tube placement and a property of water to exhibit a natural stratification effect in response to density and temperature gradients [15], this cooling method was regarded as a counter flow heat exchanger, where the two streams—vapour and cooling water—move in opposite directions.

As the vapour tube entered the tank from above, the largest part of latent and sensible heat was released into the upper tank region. Within the 3 m length of copper tube, the vapour temperature was reduced from 53.8˚C at the inlet to 16˚C at the tube outlet, only slightly higher than the ambient temperature (15.4˚C). The total enthalpy transferred into the cooling tank during the one-hour measurement period was 217 kJ (Eq. (5); $\Delta h_{inlet/outlet}$). By rearranging the specific heat capacity equation (Eq. (1)) for ΔT, it was found that if the heat had been distributed evenly, the average temperature increase in the cooling tank would only be 0.32˚C. In reality, however, the main deposition of heat occurred in the upper tank region (Fig. 3) and only a very small temperature increase was observed at the bottom of the tank during the measuring period, confirming the temperature stratification effect that developed.

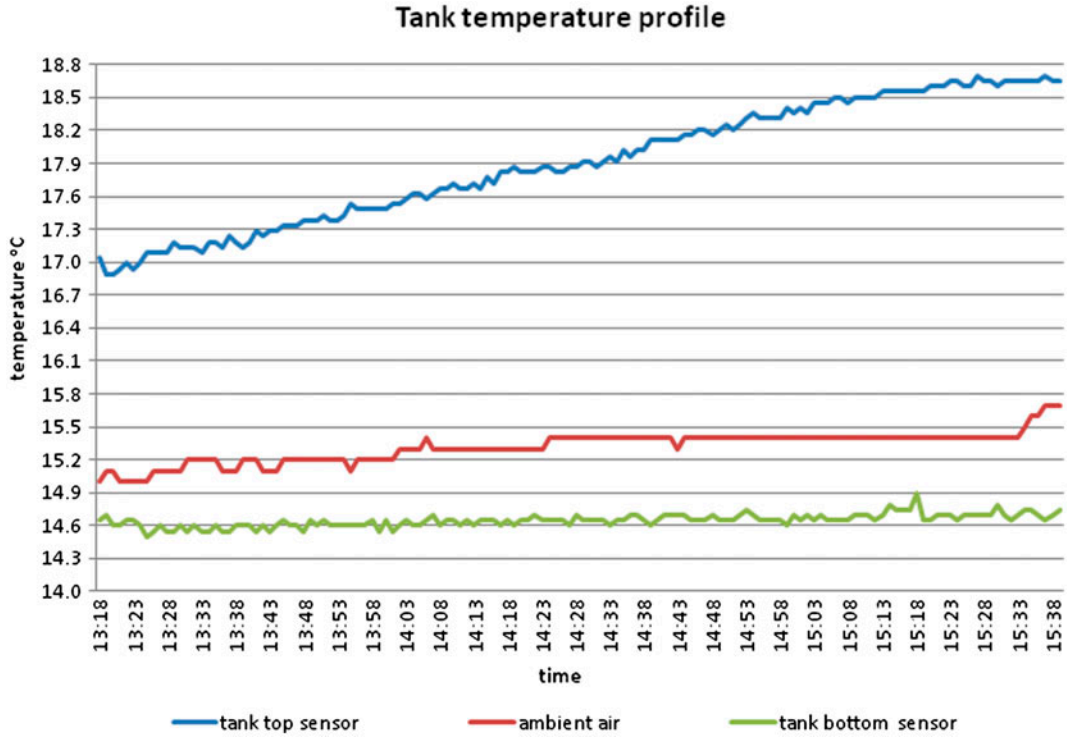

Fig. 3. Temperature increase in response to the stratification effect in the cooling tank (note that at entry point "13:18", the experiment had been running for nearly three hours).

While a more detailed description of the temperature distribution in the tank would require further investigation and is outside the scope of this paper, these results suggest some potential for latent heat recovery with minimum technical difficulty. The stratification effect could be utilised by continuously cycling the warmest water away from the upper tank region and extracting the sensible heat along the way. In an industrialised setting, this could be achieved by cycling the water through a passive radiator type air heater, where it would be cooled and re-fed into the lower tank region. The regenerative blowers used to supply air to the bubble columns would be placed in such a way that they drag ambient air through the radiator array. By preheating the air stream previous to entering the evaporator bubble column, some sensible heat from the tank water cycle would be reused.

The following section on modelling the cooling tank size is based on a conceptual bubble greenhouse with an assumed water production rate of 8 m^3 per day [24]. Extrapolated from the evaporation rate that was achieved with the laboratory-scale bubble column (with a sinter area of 78.5 cm^2 and an airflow rate of 0.81 $m^3 h^{-1}$), the total column sinter surface area required for evaporation of 8 m^3 of saltwater at a process temperature of 80°C would be 12.9 m^2. This would require a large number of columns (e.g. 70 columns with a sinter area of 1,850 cm^2 or 49 cm diameter each), to be organised in a modular configuration. The 70 columns could be arranged in 7 modules, with a series of 10 bubble columns per module. Each of the seven modules would be cooled by an individual cooling tank.

Total airflow demand per module would be 190 $m^3 h^{-1}$. A typical regenerative blower such as Republic HRB 402/1, running at 1.65 kW, produces an airflow rate of 192 $m^3 h^{-1}$ and a working pressure of 343 mbar [17]. One of these blowers could supply air to 10 bubble columns in series, each up to 30 cm high. At a column process temperature of 80°C, the total energy requirement for air pumping would be about 3.4 kW h m^{-3} of water produced, less than best practice thermal desalination processes (using vapour compression) that operate at about 4 kW h m^{-3} [25]. Total bubble column evaporation per module would be 55 L h^{-1} (1.3 $m^3 d^{-1}$). Assuming there was little heat loss between bubble column output and cooling tank inlet, the temperature at the cooling tube inlet would be close to 80°C. Total enthalpy contained in the 55 L h^{-1} of condensable water vapour per cooling tank would be 115 MJ h^{-1}. At an ambient temperature of 35°C and an optimal vapour temperature reduction to

this point, the enthalpy contained in the "vapour-to-greenhouse" stream would be 19 MJ h^{-1} (in 7.5 L h^{-1}) and the amount of heat released into the tank from condensation and cooling of 48 L h^{-1} would be 96 MJ h^{-1}.

As an approximation, using the ΔT_{in}, ΔT_{out} and LMTD relationship from the experimental data and extrapolating for a steam inlet temperature ($T_{h,in}$) of 80℃ and cooling water ($T_{c,in}$) of 35℃ from below, the cooling water temperature in the highest region of the tank ($T_{c,out}$) would be 55℃ and the steam temperature leaving the tank ($T_{h,out}$) would be 37℃. Assuming that the cooling water was constantly removed from the top, the water flow rate needed to carry away this heat would be 1.13 m^3 h^{-1} (Eq. (1)). However, there exists a strong limitation to the recovery of sensible heat in this system as a result of the significantly inferior heat capacity of air compared to water. As the 190 m^3 of air required per hour for the bubbling process would be heated by dragging it through the radiator array, due to its weight of around 228 kg and its low specific heat capacity of 1.006 kJ kg^{-1} $℃^{-1}$, there would not be enough airflow to recover sufficient amounts of energy. Of the 96 MJ h^{-1} cycled away from the tank, only 12 MJ or 13% of energy would be reused in this way (Eq. (1)). Based on this, the use of air as a heat recovery medium would be too inefficient and a more sophisticated cooling tank design would be required for improved heat recovery and thus, for a more economical bubble-greenhouse concept. Note that the conventional recovery method of using heated cooling water to feed the evaporator is only viable in true counter-flow heat exchangers, where the active transport of heat away from the hot fluid results in much less cold fluid demand. Due to the strong mismatch of water volumes in the laboratory experiment (160 L of cooling water vs. 80–88 ml h^{-1} of evaporator refill) it is not a viable option here.

3.2.3. Glass bubble column condenser

In the presence of a non-condensable carrier gas such as air, diffusion resistance to transport vapour through the non-condensable gas/vapour mixture strongly diminishes condensers' efficiency [23]. Heat transfer rates (HTR) for surface condensers can be two orders of magnitude lower than pure vapour systems, with an equivalent heat transfer coefficient as low as 1 W m^{-1} $℃^{-1}$. Consequently, surface condensers require a large heat transfer area to be effective. Condensing vapour in a water column rather than on a condenser surface can substantially improve the HTR. In a bubble column, the large condensing surface is provided by a continuously renewed air/water interface, in permanent motion due to the oscillating nature of upwards rising bubbles. For that reason, diffusion resistance is significantly reduced and strongly improved heat and mass transfer rates can be realised albeit the presence of non-condensable gas [23].

In order to assess the effectiveness of the concept, a chromatography column was modified into a simple glass column condenser (*cooling column*). It contained a sintered disk with a pore size of 40–100 μm that produced a fine bubble stream to oscillate upwards. As the cooling column was filled with deionised water, bubble coalescence was not inhibited in this environment and the bubbles created by the process were larger than in saltwater. While this resulted in a considerably smaller air/water interface in the cooling column compared to the evaporator column, it nonetheless provided a large condensation surface for water vapour to return to liquid phase. Closely correlated with theoretical condensation rates, with increasing cooling effort, condensate recovery rates of 51% for *no cooling*, 68% for *moderate cooling* and 73% for *strong cooling* experiments were recorded.

Under strong cooling conditions, rapid cooling of the vapour stream to 25.9℃ occurred almost immediately within a very short distance. Throughout the remainder of the cooling column, only a modest further temperature reduction to 25.0℃ was observed. This suggests that a much shorter cooling column with perhaps no more than 50 mm height could be equally effective under similar cooling conditions. For both the *moderate* and *strong cooling* experiments, a cooling sleeve temperature increase from bottom to top was observed, demonstrating the development of a temperature gradient similar to the previous tank concept. This was different for the *no cooling* (*passive sleeve*) experiment, where the temperature at *cool-sleeve top* was 0.2℃ lower than *cool-sleeve mid*, indicating some process that had somehow counteracted the establishment of the temperature gradient in this upper region.

The latent heat released from condensation of 58.6 g of water during the final one-hour block in the *strong cooling* experiment was 132 kJ. It can be assumed that the majority of this heat was conducted through the glass wall into the cooling sleeve and then carried away with the circulating ice water. In contrast, the 93 kJ of heat released in the *no cooling* experiment (from condensation of 41.2 g of water) was first conducted into the non-circulated or *passive sleeve* water, from where secondary heat release occurred as (a) conduction through the PVC sleeve wall and (b) over the water surface at the uncovered sleeve top. Noteworthy, the previously mentioned effect that

seemed to have counteracted the establishment of the temperature gradient in the upper sleeve region, caused the temperature at *cool-sleeve top* to plateau at around 43.2℃, more than 10℃ below the *cooling column inlet* temperature of 53.5℃ (Fig. 4). As a result of this anomaly, an impressive 51% of the evaporated water could passively be recovered from condensation.

In the upper region of the cooling sleeve, starting from the water surface down to approximately 30–40 mm below surface, the formation of air bubbles around the glass column wall was observed. This process, known as nucleate bubble formation [26], was caused by the existence of metastable gas cavities on the glass surface. Under the supersaturation conditions caused by constant heat input into the cooling sleeve water, bubbles continuously formed and grew. Simultaneously, a quantity of cooling sleeve water vaporised into the bubbles and produced an evaporative cooling effect around the outside of the glass column. With bubbles detaching and rising to the surface with some regularity, a considerable amount of heat was released from the cooling sleeve water surface in this way. While the overall performance of the *passive sleeve* glass cooling column was controlled by the temperature difference between the incoming vapour from the evaporator column and the ambient air, the heat released through nucleate bubble formation—a process that could perhaps best be described as a "self-cooling effect"—was presumably due to the particular design of the apparatus.

3.2.4. Copper bubble column condenser

The underlying motivation for the stacked column array had been to utilise the relatively large air/liquid interface as created by the bubble process for condensation and to investigate whether effective cooling could be achieved within a relatively small vessel, thus making a short bubble column condenser advantageous over a simple flat-plate condenser previously assessed [27]. As shown above, the condensing capability of an actively cooled glass column came at the cost of considerable cooling and pumping demand, in addition to an already increased air pumping requirement to overcome the hydrostatic water pressure of the stacked evaporator/cooling column array. In terms of condensation output, no significant improvement of the cooling column over the flat-plate condenser could be demonstrated.

Since the *passive sleeve* or *no cooling* column demonstrated only a relatively modest vapour temperature reduction of around 10℃, it would not be an effective vapour cooling device for the purpose of greenhouse

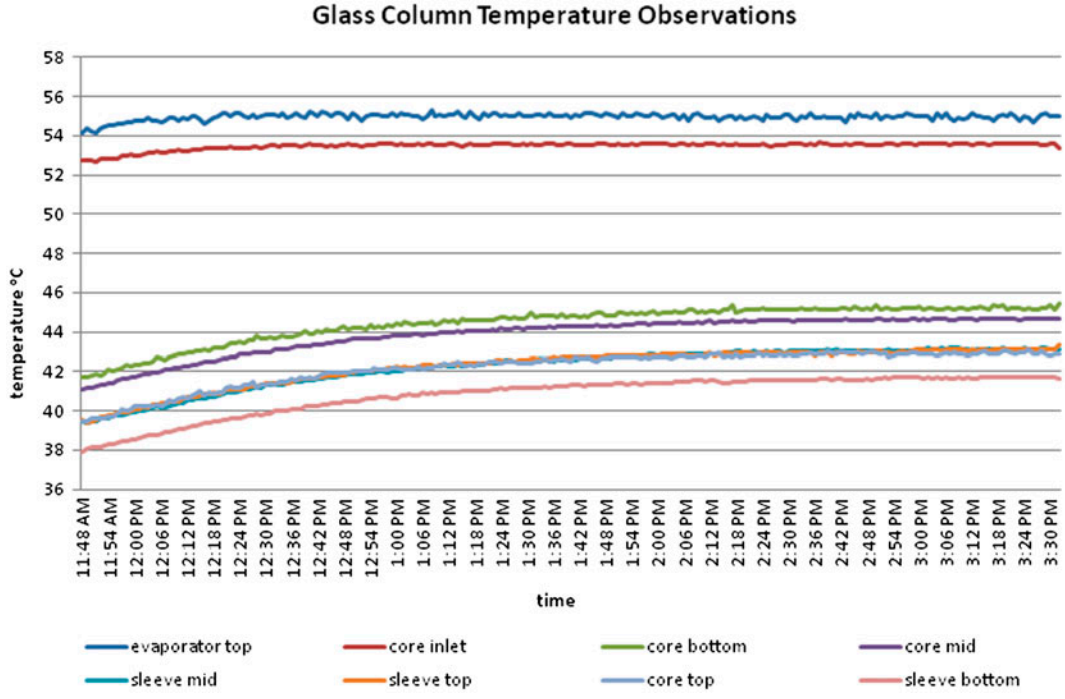

Fig. 4. Thermocouple readings for the *no cooling* glass column experiment; *sleeve top* temperature maintained 10℃ below *core inlet* temperature, representing the "self-cooling effect".

humidification. However, based on the observed "self-cooling" effect, a stacked evaporator/condenser module could perhaps hold some potential as a standalone small-scale desalination method, where the focus was simply on energy efficient condensation. It was therefore decided to investigate the concept further by substituting the glass cooling column with a modified copper column, based on the vastly larger thermal conductivity of copper (401 W m^{-1} ℃$^{-1}$) over glass (1.05 W m^{-1} ℃$^{-1}$) and its superior HTR.

Initially, the performance of an un-sleeved copper column was assessed under air-cooled conditions. While the temperature difference between *cooling column inlet* and *ambient air* was relatively large (32.7℃), the total vapour temperature reduction over the length of the column was only 10.7℃. This resulted in a low condensate recovery rate of 36% (29.7 ml), likely caused by the considerably lesser heat capacity of the cooling medium air compared to water (1.01 kJ kg^{-1} ℃$^{-1}$ vs. 4.18 kJ kg^{-1} ℃$^{-1}$) and the vertical orientation of the cooling column that limited the movement of warmed ambient air away from the copper surface. Nevertheless, encouraged by the promising condensate recovery rate of over 51% that was achieved with the *passive sleeve* glass column, a PVC sleeve was fitted in a similar manner to the copper column. In *passive sleeve* mode, the condensation rates recorded for glass (41.2 ml) and copper (42.0 ml) columns were fairly similar and nucleate bubble formation was also observed around the copper column. However, the copper column demonstrated a faster initial temperature reduction at the inlet location which correspondingly suggested an increased heat input into the cooling sleeve. Contradictory, all of the *cool-sleeve* sensor locations showed a significantly lower temperature than in the glass column experiment which would require a faster heat release to the ambient air and away from the cooling sleeve itself. The temperature at *cool sleeve top* levelled at around 41.0℃, more than 11℃ below the *cooling column inlet* temperature of 52.1℃. This suggests a slightly stronger heat release effect through the nucleate bubble formation process. Notwithstanding this, the relatively small condensate gain over the glass column did not reflect the vastly superior heat transfer capacity of copper.

3.3. Condenser effectiveness

All of the concepts assessed in this paper essentially represented simple embodiments of compact heat exchangers. For a better comparison of the different approaches to the vapour cooling task, the *effectiveness*–NTU method was used [19]. Effectiveness (ε) is the actual heat transferred, divided by the maximum heat that could possibly be transferred from one stream to the other (q/q_{max}). The tube-based devices resembled shell and tube-type heat exchangers, whereas the bubble columns fell under the category of direct contact heat exchangers. In their air-cooled embodiments where heat transport relied on natural convection, the copper tubes and the copper column were neither truly parallel nor counter flow, however they were considered closer to parallel flow in that the air surrounding the tube at the inlet was much warmer than the air around the tube outlet position (with a gradual temperature reduction along the way). All water-cooled devices were considered as counter flow, based on the temperature stratification that developed in the cooling sleeve and cooling tank.

In order to define the effectiveness of a heat exchanger, an energy balance allows calculating the maximum possible heat transfer that can be hypothetically achieved. As the cold stream mass flow could not be practically measured in the air-cooled and *passive sleeve* experiments, it was calculated by considering the heat lost by the hot fluid and the heat gained by the cold fluid to be in a balanced relationship. The energy balance (Eq. (4)) can be solved for one unknown variable, in this case for the cold stream mass flow rate M_c (Table 2; Column 8). Mass heat capacity C_h used in the equation was calculated by subtracting the enthalpy of moist air (Eq. (5)) at the respective cooling device's vapour inlet point ($T_{h,in}$) from the enthalpy of moist air at its vapour outlet point ($T_{h,out}$). As there was no active transport of heat away from the air-cooled devices, large amount of air needed to be replaced by passive forces, i.e. rising of warm air away from the condenser and upwards into the room. This process was strongly limited by the much smaller "footprint" of the vertically placed copper column and the correspondingly low amount of air movement, compared to the horizontally placed 3 m long copper tubes with a much larger "footprint" area (Table 2; Column 9).

For the *passive sleeve* glass and copper columns, the theoretical amount of cooling water required to transport away the heat would be 18 and 11 L, respectively. However, as there was no actual cooling water exchange, heat removal occurred by means of the previously mentioned "self-cooling" effect. For the moderate and strong cooled glass column experiments where there was cooling water circulation, only a slightly higher amount of 19 and 22 L, respectively (compared to the 18 L in *passive sleeve*), was calculated. This suggested that the added expenditure for water circulation was not justified and a well-designed passive sleeve concept could be a cost-effective low key method.

Table 2
Mass (weight and volume) flow rates, heat capacities and hot and cold temperatures of individual condenser streams (C_h and C_c are in kJ kg^{-1} C^{-1})

	M_h (kg h^{-1})	C_h	$T_{h,in}$ (°C)	$T_{h,out}$ (°C)	C_c	$T_{c,in}$ (°C)	$T_{c,out}$ (°C)	M_c (kg h^{-1})	Vol_c (m^3 h^{-1})
Copper tube type I	0.97	159.4	52.9	28.8	1.006	19.2	26.3	523	436
Copper tube type II	0.97	177.9	53.5	26	1.006	16.2	23.9	614	512
Type II in cooling tank	0.97	213.2	53.8	16	4.181	13.8	29.1	122	0.122
Glass col. passive sleeve	0.97	80.7	53.5	43.9	4.181	41.8	43.2	129	0.129
Glass col. moderate cool	0.97	149.3	53.5	32.2	4.181	25.2	31.5	117	0.117
Glass col. strong cool	0.97	184.2	53.7	25	4.181	13.6	23.6	123	0.123
Copper col. passive sleeve	0.97	81.2	52.1	42	4.181	38.6	41	79	0.079
Copper col. air cooling	0.97	49.3	51.9	46	1.006	19	24.2	54	45
Flat-plate condenser[a]	0.97	182.0	53.3	24.3	1.006	17	33.7	305	254

[a]Flat-plate condenser in air-cooled mode [27].

In order to calculate the overall heat transfer coefficient (U), the heat capacity rates C_h (hot stream) and C_c (cold stream) were calculated by multiplying the mass flow rate (m) of the fluid (in kg h^{-1}) with the mass heat capacity (C) of the fluid (in kJ kg^{-1} C^{-1}). C_{min} is denoted as the smaller value of C_h and C_c. In all cooling concepts presented, C_h equalled C_{min}, which allowed for the terms to be omitted from the effectiveness equation (Eq. (6)). By calculating effectiveness (Eq. (6)), followed by NTU calculation (Eq. (7)) and (Eq. (8)), the overall heat transfer coefficient for all tested devices was determined (Table 3).

Compared to commercial steam radiators (U = 5–20), air heaters (U = 10–50) or industrial condensers (U > 1,000) [28], all the tested devices had very low heat transfer coefficients. In praxis however, the overall heat transfer U is strongly influenced by the volume of the hot stream and moreover, by a well-matched relationship between hot and cold flows. In the laboratory set-up, very low amounts of steam (0.97 kg h^{-1}) were processed, compared to the significantly larger inputs in commercial applications. If for example, the vapour flow (M_h) rate was increased by an order of magnitude, the cold flow rate and U would increase by the same factor (calculated by using Eqs. (4), (6)–(8)).

With this in mind, the tested devices aimed at achieving a reasonable cooling effect and condensation "return" in passive mode, without particular consideration for the matching of streams, for example, by utilising natural convection of an unspecified amount of air that can freely move away from the copper tubes. Of all air-cooled devices, the best results were achieved by the narrow type I tube, while type II was less effective (Table 3), based on the factors outlined above (Section 3.2.1). The air-cooled copper bubble condenser was inferior to the tubes, due to its vertical placement and a resulting smaller heat release footprint that limited heat removal by free air convection.

Table 3
Comparison of effectiveness and overall heat transfer coefficient (U) for individual cooling concepts; c = counter flow/(p) = parallel flow

	C_h (W K^{-1})	C_c (W K^{-1})	C_{min} (W K^{-1})	C_{ratio}	ε	A (m^2)	NTU c/(p)	U c/(p)
Copper tube type I	0.043	0.146	0.043	0.29	0.72	0.06	1.4 (2.0)	1.04 (1.44)
Copper tube type II	0.048	0.172	0.048	0.28	0.74	0.12	1.5 (2.2)	0.61 (0.90)
Type II in cooling tank	0.058	0.142	0.058	0.40	0.95	0.12	4.1 (na)	1.95 (na)
Glass col. passive sleeve	0.023	0.149	0.023	0.15	0.82	0.06	1.9 (2.5)	0.68 (0.89)
Glass col. moderate cool	0.040	0.136	0.040	0.30	0.75	0.06	1.6 (2.9)	1.09 (1.92)
Glass col. strong cool	0.050	0.143	0.050	0.35	0.72	0.06	1.5 (2.5)	1.24 (2.06)
Copper col. passive sleeve	0.022	0.092	0.022	0.24	0.75	0.04	1.6 (2.1)	0.85 (1.15)
Copper col. air cooling	0.013	0.015	0.013	0.88	0.18	0.04	0.2 (0.2)	0.07 (0.07)
Flat-plate condenser[a]	0.049	0.085	0.049	0.58	0.80	0.15	2.3 (na)	0.76 (na)

[a]Flat-plate condenser in air-cooled mode [27].

Table 4
Summary of temperature changes and endpoint vapour temperatures for individual pre-cooling devices

Cooling type	Copper tube type I air cooling	Copper tube type II air cooling	Copper tube type II passive tank cooling	Glass column passive sleeve	Copper column air cooling	Copper column passive sleeve
Bubble column top temperature in ℃	54.1	54.3	54.5	55.0	53.9	54.3
Exhaust vapour temperature in ℃	28.8	26.0	16.0	43.9	46.0	42.0
Ambient temperature in ℃	18.8	16.1	15.4	25.4	19.2	19.8
ΔT from column top to exhaust; in ℃	25.3	28.3	38.5	12.1	7.9	12.3
ΔT from exhaust to ambient; in ℃	10.0	9.9	0.6	17.5	26.8	22.2

The best heat transfer rate overall was achieved with the tube in tank design but the outcome was heavily biased by the mismatch between the hot vapour stream and the considerably oversized cooling stream (i.e. tank content). For a vapour stream several orders of magnitude larger, as is required for a conceptual bubble greenhouse, this ratio would be impossible to maintain. On the other hand, the compact water-cooled bubble columns were relatively effective and in order to increase their HTR while simultaneously maintaining their simplicity, adjustment of hot and cold mass flow rates would further improve their performance, for example by increasing the cooling water cycling rate, albeit the cost of additional energy use for cooling and pumping. The observed "self-cooling" of the passive sleeve concept that could not be further examined within the timeframe of this study, suggest for now a unexplained mechanism that may hold great potential for passive condensation in small-scale desalination systems, particularly under higher vapour temperature conditions, where a presumed 10℃ drop would produce distinctly higher yields than those achieved under the conditions of around 53℃ reported here.

3.4. Suitability of individual passive cooling concepts for greenhouse vapour pre-treatment

Besides determining their ability to produce condensate, the primary motivation for this research was to assess the vapour cooling concepts in terms of their vapour temperature reduction potential. Of the passive devices, the air-cooled copper tubes achieved considerable temperature reductions of 25–28℃ under the ambient conditions of around 16–19℃ (Table 4). However, their cooling ability would be diminished when considering two important aspects. First, in an open environment the ambient temperatures could be much higher depending on the location of a full-scale bubble greenhouse and second, in order to increase the system productivity, the bubble column would ideally be operated at a significantly higher temperature than the 55℃ tested here.

Under the prevailing ambient laboratory conditions of 15.4℃, the cooling tank system could achieve a total temperature reduction of 38.5℃, with a vapour exhaust temperature just above ambient level. This would not only be safe for the primary purpose of greenhouse humidification, but could also be tailored as a standalone approach to air conditioning the greenhouse when required. However, up-scaling this system into a larger bubble greenhouse would only be feasible with an efficient heat extraction design as highlighted above. The passive glass and copper column condensers were generally not found capable of reducing vapour temperature sufficiently, neither in sleeved nor un-sleeved mode. Under ambient temperatures of around 20–25℃, only modest vapour temperature reduction in the range of 8–12℃ could be achieved. Importantly, the two factors (1) elevated ambient temperatures depending on location and (2) higher bubble column operating temperatures would be equally detrimental to their performance.

Notwithstanding their limited effectiveness for vapour cooling purposes, most of the tested devices demonstrated some potential as the condensing component for a standalone bubble column-based small-scale desalination system, perhaps substituting a conventional solar still. Based on their passive operation and technical simplicity, their limited water production rate would be acceptable where brackish water and sunshine are abundant. While the air-cooled devices would be strongly influenced by the ambient temperature at particular locations, the "self-cooling" sleeve concept could potentially offer an

ambient independent solution that warrants further investigation. The passive cooling tank concept with its impressive condensate recovery rate of over 80% could perhaps be expanded into a larger system, where a substantial water tank (e.g. water storage for dust suppression purpose in mining operations) could act as an oversized heat sink.

4. Conclusion

The findings presented here provide valuable insights into low-key passive cooling methods and their heat exchange ability and thus, inform the conceptualisation of a bubble-greenhouse desalination system. While the investigated devices were based on a number of different physical concepts, their common feature was the necessity for effective cooling under the proviso of relatively low-energy demand for the component itself. Furthermore, they should be easy to manufacture, of low investment cost, economically feasible and technically and operationally appropriate for local people in remote places.

For the purpose of cooling bubble column vapour to acceptable greenhouse temperatures, most of the passive devices could not deliver the desired results. While the copper tube prototypes achieved promising water recovery rates and temperature reductions under laboratory conditions, elevated ambient air temperatures would be detrimental to their productivity. Therefore, the concept might only be conditionally suitable, for example during cooler seasons or when utilised in generally colder desert climates. Further research into the tube concept could lead to innovative designs, where cooling tubes were placed below the ground surface to utilise the cooler soil temperatures or buried into the natural slope of a hill to utilise gravity for unforced condensate outflow.

All tested devices represent a single-stage approach to thermal desalination and may therefore only be valid in a larger setting where free heat, e.g. from industrial combustion processes, is available. Otherwise, a well designed latent heat recovery system would be crucial for the economic feasibility of a bubble greenhouse. To some degree, heat recycling would be possible with a relatively simple cooling tank design, where a circulation system extracts heat from the tank and makes it available for the evaporation process via the air bubbling process. By varying dimensions, circulation rates, etc., a cooling tank design could perhaps be tailored to mitigate the vapour for safe greenhouse humidification. To that end, future work should focus on improving the heat recovery concept, ideally by direct heat transfer via the recovery cycle into the bubble column evaporator.

The stacked evaporator/condenser bubble column array, thought to be advantageous due to its large air/water interface, did not demonstrate a significant cooling/condensing advantage over a simple flat-plate homemade condenser. However, the observed "self-cooling" effect could perhaps be utilised to produce small quantities of potable water in hot and arid regions, as a simple alternative to conventional solar stills. Despite the limited condensation and cooling ability of the stacked evaporator/condenser bubble module, further research of the concept is warranted based on its potential for passive condensation.

Finally, while thermal desalination systems such as the conceptual bubble greenhouse have a high energy demand, their main focus is on participation and the involvement of local people in process operation, maintenance and repair. Herein lies its advantage over conventional water treatment methods like reverse osmosis, as its simplicity translates into numerous social benefits such as capacity building, self determination and empowerment of people in remote locations. Putting a monetary value on these communal benefits will allow offsetting the cost of water production from alternative but ultimately, sustainable schemes.

List of symbols

A	—	surface area in m^2
C	—	specific enthalpy of condensation (heat capacity) in kJ kg^{-1} C^{-1}
C_h and C_c	—	mass heat capacity of the hot and cold fluid in kJ kg^{-1} C^{-1}
C_{min}	—	smaller value of C_h (hot stream) and C_c (cold stream)
c_{pa}	—	specific heat capacity of air (1.006 kJ kg^{-1} $°C^{-1}$)
c_{pw}	—	specific heat of water vapour at constant pressure (1.875 kJ kg^{-1} $°C^{-1}$)
C_{ratio}	—	C_{min}/C_{max}
ε	—	effectiveness
h_m	—	enthalpy of moist air
h_{we}	—	evaporation heat of water at 0°C (2,501 kJ kg^{-1})
m	—	mass flow rate per time in kg s^{-1}
m_h and m_c	—	mass flow rate of the hot and cold fluid in kg h^{-1}
NTU	—	number of transfer units
Q	—	rate of heat transfer in kJ s^{-1}
T	—	air temperature (in °C, relative to zero)
$T_{c,in}$ and $T_{c,out}$	—	inlet and outlet temperatures on exchanger cold side in °C
$T_{h,in}$ and $T_{h,out}$	—	inlet and outlet temperatures on exchanger hot side in °C
ΔT	—	temperature change in °C
$\Delta T_{in,counter\ flow}$	—	$t_{h,in} - t_{c,out}$ (inlet hot and outlet cold stream in °C)

$\Delta T_{in,parallel\ flow}$ — $t_{h,in} - t_{c,in}$ (inlet hot and inlet cold stream in ℃)
ΔT_{mean} — logarithmic mean temperature difference (LMTD)
$\Delta T_{out,counter\ flow}$ — $t_{h,out} - t_{c,in}$ (outlet hot and inlet cold stream in ℃)
$\Delta T_{out,parallel\ flow}$ — $t_{h,out} - t_{c,out}$ (outlet hot and outlet cold stream in ℃)
U — overall heat transfer coefficient
x_s — humidity ratio at saturation in kg of water per kg of air

References

[1] S.A. El-Agouz, A new process of desalination by air passing through seawater based on humidification–dehumidification process, Energy 35(12) (2010) 5108–5114.
[2] E.W. Tow, J.H. Lienhard V, Experiments and modeling of bubble column dehumidifier performance, Int. J. Therm. Sci. 80 (2014) 65–75.
[3] G.P. Narayan, G.P. Thiel, R.K. McGovern, J.H. Lienhard, M.H. Elsharqawy, Bubble-Column Vapor Mixture Condenser, US Patent 8,523,985, 2013.
[4] G.P. Narayan, K.M. Chehayeb, R.K. McGovern, G.P. Thiel, S.M. Zubair, J.H. Lienhard V, Thermodynamic balancing of the humidification dehumidification desalination system by mass extraction and injection, Int. J. Heat Mass Transfer 57(2) (2013) 756–770.
[5] K.M. Chehayeb, G.P. Narayan, S.M. Zubair, J.H. Lienhard V, Use of multiple extractions and injections to thermodynamically balance the humidification dehumidification desalination system, Int. J. Heat Mass Transfer 68 (2014) 422–434.
[6] S. Jackson, Indigenous Interests and the National Water Initiative (NWI): Water Management Reform and Implementation, in CSIRO. Sustainable Ecosystems Report for NAILSMA's Indigenous Water Policy Group, North Australian Indigenous Land and Sea Management Alliance, Darwin, 2007.
[7] R. Ouahes, C. Ouahes, P. Le Goff, J. Le Goff, A hardy, high-yield solar distiller of brackish water, Desalination 67 (1987) 43–52.
[8] U. Oztoker, M.K. Selcuk, Theoretical Analysis of a System Combining a Solar Still with a Controlled-Environment Greenhouse, American Society of Mechanical Engineers, New York, NY, Medium: X; Size: Pages: 12, 1971.
[9] S.M. El-Haggar, A.A. Awn, Optimum conditions for a solar still and its use for a greenhouse using the nutrient film technique, Desalination 94(1) (1993) 55–68.
[10] N.S.L. Srivastava, M. Din, G.N. Tiwari, Performance evaluation of distillation-cum-greenhouse for a warm and humid climate, Desalination 128(1) (2000) 67–80.
[11] M.T. Chaibi, T. Jilar, System design, operation and performance of roof-integrated desalination in greenhouses, Solar Energy 76(5) (2004) 545–561.
[12] M.T. Chaibi, T. Jilar, Effects of a solar desalination module integrated in a greenhouse roof on light transmission and crop growth, Biosyst. Eng. 90(3) (2005) 319–330.
[13] C. Paton, P.A. Davis, M.F.A. Goosen, S.S. Sablani. Seawater greenhouse development for Oman: Thermodynamic modelling and economic analysis, 2001. Available from: <http://www.seawatergreenhouse.com/downloads/MEDRC%20Report%20-%20Seawater%20Greenhouse%20Development.pdf> (31 May 2010).
[14] S.S. Sablani, M.F.A. Goosen, C. Paton, W.H. Shayya, H. Al-Hinai, Simulation of fresh water production using a humidification-dehumidification seawater greenhouse, Desalination 159 (2003) 283–288.
[15] H. Mahmoudi, N. Spahis, S.A. Abdul-Wahab, S.S. Sablani, M.F.A. Goosen, Improving the performance of a Seawater Greenhouse desalination system by assessment of simulation models for different condensers, Renew. Sustainable Energy Rev. 14(8) (2010) 2182–2188.
[16] C.R. Nave, Empirical Fit of Saturated Vapor Density versus Celsius Temperature, 2012. Available from: <http://hyperphysics.phy-astr.gsu.edu/hbase/kinetic/relhum.html> (18 February 2015).
[17] M.J. Francis, R.M. Pashley, Thermal desalination using a non-boiling bubble column, Desalin. Water Treat. 12 (1–3) (2009a) 155–161.
[18] A.M. Radhwan, H.E.S. Fath, Thermal performance of greenhouses with a built-in solar distillation system: Experimental study, Desalination 181 (2005) 193–205.
[19] J.H. Lienhard IV, J.H. Lienhard V, A Heat Transfer Textbook, fourth ed., Phlogiston Press, Cambridge, Massachusetts, 2012.
[20] B. Bouchekima, A solar desalination plant for domestic water needs in arid areas of South Algeria, Desalination 153(1–3) (2002) 65–69.
[21] G.P. Narayan, M.H. Sharqawy, E.K. Summers, J.H. Lienhard, S.M. Zubair, M.A. Antar, The potential of solar-driven humidification–dehumidification desalination for small-scale decentralized water production, Renew. Sustainable Energy Rev. 14(4) (2010) 1187–1201.
[22] S.A. El-Agouz, M. Abugderah, Experimental analysis of humidification process by air passing through seawater, Energy Convers. Manage. 49(12) (2008) 3698–3703.
[23] G.P. Narayan, J.H. Lienhard V, Thermal design of humidification–dehumidification systems for affordable small-scale desalination, IDA J. Desalin. Water Reuse 4(3) (2012) 24–34.
[24] M. Schmack, G. Ho, M. Anda, The bubble-greenhouse: A holistic sustainable approach to small-scale water desalination in remote regions, Desalination 365 (2015) 250–260.
[25] J.E. Miller, Review of Water Resources and Desalination Technologies, 2003. Available from: <http://prod.sandia.gov/techlib/access-control.cgi/2003/030800.pdf> (17 March 2015).
[26] S.F. Jones, G.M. Evans, K.P. Galvin, Bubble nucleation from gas cavities—A review, Adv. Colloid Interface Sci. 80(1) (1999) 27–50.
[27] M. Schmack, G. Ho, M. Anda, A bubble column evaporator with basic flat-plate condenser for brackish and seawater desalination, Environ. Technol. (2015) 1–12.
[28] F. Kreith, R. Manglik, M. Bohn, Principles of Heat Transfer, Cengage Learning, Stamford, 2010.